Jul 1st, 12:00 AM

Large-Eddy Simulation of Pollutant Dispersion in Downtown Montreal: Evaluation of the Convective and Turbulent Mass Fluxes

Pierre Gousseau

Bert Blocken

Ted Stathopoulos

GertJan van Heijst

International Environmental Modelling and Software Society (iEMSs)
2012 International Congress on Environmental Modelling and Software
Managing Resources of a Limited Planet, Sixth Biennial Meeting, Leipzig, Germany
R. Seppelt, A.A. Voinov, S. Lange, D. Bankamp (Eds.)
http://www.iemss.org/society/index.php/iemss-2012-proceedings

Large-Eddy Simulation of Pollutant Dispersion in Downtown Montreal: Evaluation of the Convective and Turbulent Mass Fluxes

Pierre Gousseau[a], Bert Blocken[a], Ted Stathopoulos[b], GertJan van Heijst[c]
[a]*Unit Building Physics and Services, Department of the Built Environment, Eindhoven University of Technology, Eindhoven, The Netherlands*
[b]*Building, Civil and Environmental Engineering, Concordia University, 1455 Blvd. de Maisonneuve West, Montreal, Quebec, Canada, H3G 1M8*
[c]*Fluid Dynamics Laboratory, Department of Applied Physics, Eindhoven University of Technology, Eindhoven, The Netherlands*
p.gousseau@tue.nl

Abstract: Large-Eddy Simulation of pollutant dispersion from a stack on the roof of a low-rise building in downtown Montreal is performed. Two wind directions are considered, with different wind flow patterns and plume behaviours. The resulting mean concentration field is observed and analysed with the computed (mean) convective and turbulent mass fluxes. These two concepts allow gaining some insight into the dispersion process and analysing the deficiencies of less sophisticated turbulence models. When the emitting building is located downstream of a high-rise building (case SW), the turbulent mass flux is directed from the high to low levels of mean concentration and the gradient diffusion hypothesis often used with steady models is verified. However, when the influence of the surrounding buildings is smaller (case W), a counter-gradient mechanism is observed in the streamwise direction, confirming the results obtained on isolated buildings. The present study supports the use of generic, simplified cases to investigate environmental processes; the conclusions can subsequently be applied to real and more complex cases.

***Keywords**:* Computational Fluid Dynamics (CFD); gas dispersion; wind flow; scalar transport.

1 INTRODUCTION

Computational Fluid Dynamics (CFD) is increasingly used and explored to investigate micro-scale wind-induced pollutant dispersion in urban environments. Because of the turbulent nature of the wind flow around buildings, the accuracy of the CFD simulations depends strongly on the turbulence modelling approach selected. In the field of wind engineering, two of them are generally used: steady Reynolds-Averaged Navier-Stokes (RANS) and Large Eddy Simulation (LES).
In turbulent flows, dispersion can be seen as the combination of convective and turbulent mass transport. The accurate prediction of the concentration field is strongly linked to the accurate prediction of each of these two components. Concerning the turbulent mass transport, RANS models generally assume that the turbulent mass flux is proportional and opposite to the gradient of mean concentration, with the so-called gradient-diffusion (GD) hypothesis: $Q_{t,i}=-D_t \times \partial C/\partial x_i$, with $Q_{t,i}$ the i-th component of the turbulent mass flux, D_t the turbulent mass diffusivity, and $C=\langle c \rangle$ the mean concentration. However, in some cases like for example dispersion from a rooftop vent on a cubical building, it appears that this

hypothesis is not valid (Gousseau et al. [2011b]). Since only the effects of the small scales of motion on the dispersion process are modelled with LES, this approach generally provides a better prediction of the turbulent mass transport and can be used to verify whether the GD hypothesis is valid or not.
This evaluation is performed in the present paper, for the case of pollutant dispersion in an actual urban environment (downtown Montreal, Canada). LES with the dynamic Smagorinsky subgrid-scale (SGS) model is used to simulate dispersion of pollutant gas emitted by a stack on the roof of a low-rise building. Two wind directions are considered. The surrounding building density is high, which makes the prediction of the concentration field particularly challenging. The configuration under study is inspired by the wind-tunnel experiments by Stathopoulos et al. [2004], which are described in the next section. Next, the numerical method is outlined and finally the results are presented and analyzed.

2 DESCRIPTION OF THE EXPERIMENTS

On-site and wind-tunnel measurements of pollutant dispersion in downtown Montreal have been performed by Stathopoulos et al. [2004]. SF_6 was used as a tracer gas and released from a stack on the roof of a three-storey building (named 'BE building') in the city center (Fig. 1).
The laboratory experiments (scale 1:200) are reproduced in this paper, for two different configurations. The first one (case SW) is for South-West wind direction, a stack height h_s = 1 m and a momentum ratio M = 5, the latter being defined as the ratio W_e/U_H with W_e the stack exhaust velocity and U_H the mean approach-flow wind velocity at building height (H). For this wind direction, the BE building is located immediately downstream of the Faubourg building (Figs. 1, 2a). The second configuration (case W) is for westerly wind direction, h_s = 3 m and M = 3 (Figs 1, 3a). In this case, the emitting building is located in the far wake of several high-rise buildings. Note that the stack location is different for both cases.

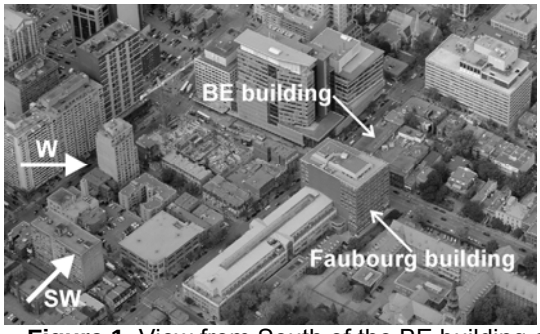

Figure 1. View from South of the BE building and its surroundings in downtown Montreal and wind directions considered in the present study.

3 NUMERICAL MODELLING

3.1 Computational Domains and Grids

The wind-tunnel experiments described above have been reproduced with the commercial CFD code Fluent 6.3. Two computational domains and grids have been created, one for each wind direction (Figs 2b, 3b). The inlet and outlet planes are perpendicular to the flow direction (x). The vertical direction is indicated by the z axis. Note that for case SW, the most upstream low-rise buildings have been assumed to have limited influence on the plume dispersion, so they have been omitted in the domain to decrease the total number of cells. In both cases, at least one street block in each direction is explicitly modelled, in agreement with the guidelines by Tominaga et al. [2008]. The domain dimensions are based on the

COST Action 732 guidelines (Franke et al. [2007]): 5 x 2.125 x 1.65 m³ for case SW and 5.75 x 2.3 x 1.65 m³ for case W (model scale dimensions).
The high-resolution computational grids are composed of hexahedral cells arranged in a horizontally-unstructured and vertically-structured way. They have been created by using the surface-grid extrusion technique by van Hooff and Blocken [2010]. They are composed of 4,791,744 and 5,257,343 cells for case SW and W, respectively. At least 10 cells are used to discretize the sides of the surrounding buildings. The ratio of two neighbouring cells dimensions is kept below 1.1. The other grid characteristics are summarized in Table 1. The conclusion of the grid-sensitivity analysis that has been conducted for case SW (see Gousseau et al. [2011a]) is that for LES the concentration values on the roof of the BE building increase slightly (on average by 11%) when a higher grid resolution is used, but it is argued that this variation does not justify the large increase in computational time required: the simulations on the fine grid were up to one month long on the fine grid, compared to two weeks on the one used here.
At the inlet of the domain, the profiles of U, k and ε are imposed, based on the wind-tunnel measurements. The mean velocity profile corresponds in both cases to a power-law ($U(z)/U_{ref}=(z/z_{ref})^{\alpha}$) with U_{ref}=12.5 m/s at z_{ref}=0.6 m and α=0.3. The time-dependent velocity profile is generated using the vortex method (Mathey et al. [2006]) with 190 vortices. The exhaust face of the stack is defined as a velocity inlet. The hydraulic diameter (0.002 m) and an assumed value of turbulence intensity of 10% (based on typical values encountered in fully-developed pipe flows) are prescribed for both cases. The top and lateral boundaries of the domain are defined as symmetry boundaries. At the outlet plane, zero static pressure is imposed. The ground and building surfaces are defined as no-slip walls: the velocity at each wall-adjacent cell's centroid is assumed to fall either in the linear sub-layer or in the logarithmic region of the boundary layer, depending on its distance to the wall (Fluent Inc. [2006]).

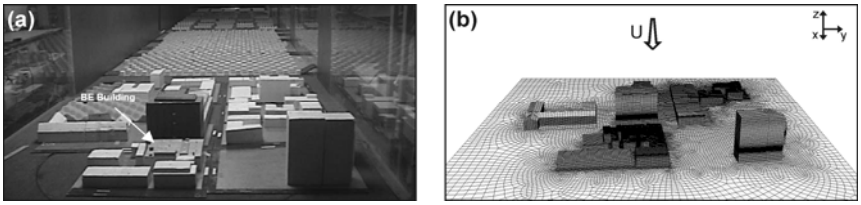

Figure 2. Case SW: (a) wind-tunnel model and (b) corresponding computational grid on the building and ground surfaces (total number of cells: 4,791,744).

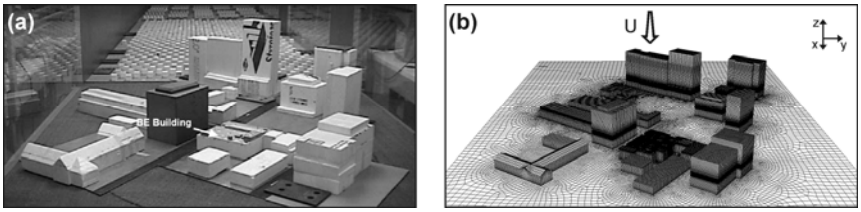

Figure 3. Case W: (a) wind-tunnel model and (b) corresponding computational grid on the building and ground surfaces (total number of cells: 5,257,343).

Table 1. Main characteristics of the computational grids. Cell sizes are expressed at model scale (1:200).

Case	Nr of cells: Total	Nr of cells: Stack circumf.	Nr of cells: BE building	Cell size at other buildings (mm)	Cell size at exterior domain boundaries (mm)
SW	4,791,744	32	130x96x49	7.5 to 15	40
W	5,257,343	32	136x104x51	7.5 to 15	40

3.2 Turbulence and Dispersion Modelling

With LES, the flow equations are filtered so that the distinction is made between the scales of motion which are smaller than the filter width (equal to the grid size in this case) and those which are larger. Only the largest scales of motion are explicitly resolved. The influence of the smallest scales on the flow is modelled here with the dynamic Smagorinsky SGS model (Smagorinsky [1963]; Germano et al. [1991]; Lilly [1992]): the Smagorinsky coefficient is computed at each time step based on the smallest resolved scales.
Dispersion of the pollutant gas is treated with the Eulerian approach: the SF_6 concentration is a scalar (c) transported by an advection-diffusion equation. Once filtered, this equation contains the so-called SGS mass flux, representing the effects of the smallest scales of motion on the resolved concentration field. It is computed via the SGS turbulent viscosity v_{SGS} and the SGS Schmidt number Sc_{SGS}, which is here determined with a dynamic procedure in the same way as the Smagorinsky constant C_s (Moin et al. [1991]).
In what follows, the mean concentration is expressed in non-dimensional form with the concentration coefficient K defined by:

$$K = \frac{\chi H^2 U_H}{Q_e} \tag{1}$$

where χ is the mean mass fraction of SF_6 and Q_e is the SF_6 emission rate (m^3s^{-1}).

On average, the pollutant transport can be decomposed into the convective ($\overrightarrow{Q_c}$) and turbulent ($\overrightarrow{Q_t}$) mass fluxes, defined by:

$$Q_{c,i} = U_i C \tag{2}$$

$$Q_{t,i} = \langle u_i' c' \rangle \tag{3}$$

The convective flux corresponds to the transport of the mean concentration C by the mean flow-field. The turbulent mass flux is due to the turbulent fluctuations of velocity ($u_i' = u_i - U_i$, with $U_i = \langle u_i \rangle$ the mean velocity component in the direction i) and concentration ($c' = c - C$). It does not take into account the SGS mass flux, which is assumed negligible. The results in the next section are presented in non-dimensional form with Q_0 the reference flux ($kg.m^{-2}s^{-1}$) defined by:

$$Q_0 = \frac{Q_e \rho_{SF_6}}{H^2} \tag{4}$$

where ρ_{SF6} is the density of SF_6.

3.3 Numerical procedure

The momentum equation is discretized with a bounded central-differencing scheme and a second-order upwind scheme is used for the energy and SF_6 concentration equations. Pressure interpolation is second order. Time integration is second order implicit. The non-iterative fractional step method (Bell et al. [1989]) is used for time advancement. The time step is set to $\Delta t = 5.10^{-4}$ s, which leads to a Courant number below 1 in the majority of the cells. The results presented hereafter have been averaged over a period of 5 s (10,000 time steps).

4 RESULTS

4.1 Mean concentration field

The contours of K in the plane aligned with the wind direction and containing the stack ($y=y_{stack}$) for the two cases under study are shown in Fig. 4. Note that the x-axis is inverted in Fig. 4b to allow visualizing the plume. For case SW (Fig. 4a), the plume is deviated towards the leeward façade of the upstream Faubourg building,

against the approach-flow wind direction. The reason is the occurrence of backflow at the source location, as will be shown later. For case W (Fig. 4b), the pollutant is mainly transported downstream by the wind flow. Note that the buildings that can be seen upstream of the BE building in Fig. 4b are outside of the plane $y=y_{stack}$ (see also Fig. 2b) and do not disturb significantly the plume. It should be noted that the comparison between numerical and experimental values of K at several (15 and 13 for case SW and W, respectively) locations on the roof of the BE building has been performed in Gousseau et al. [2011a]. Agreement was good for case SW; higher discrepancies were observed for case W, due to the deviation of the plume by the presence of a lateral velocity component at the location of the stack.

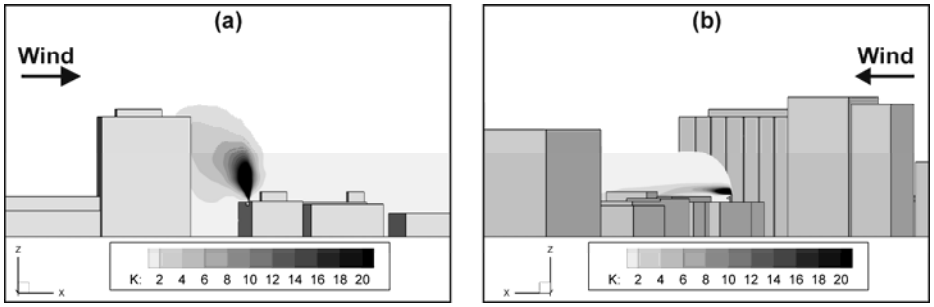

Figure 4. Contours of non-dimensional concentration coefficient K in the plane $y=y_{stack}$ for (a) case SW and (b) case W.

4.2 Case SW: mass fluxes

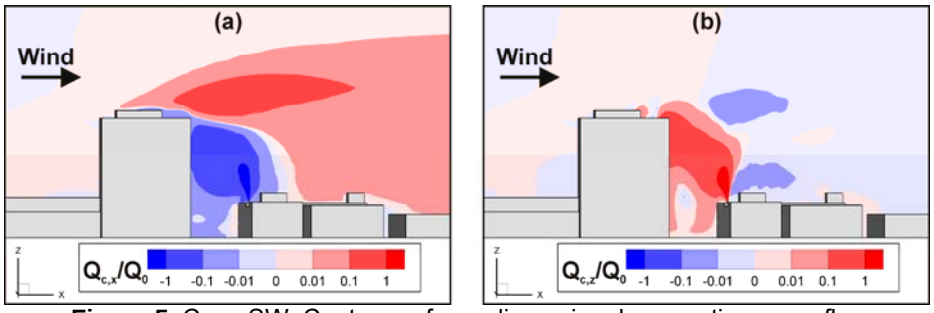

Figure 5. Case SW: Contours of non-dimensional convective mass flux components in the (a) streamwise and (b) vertical direction.

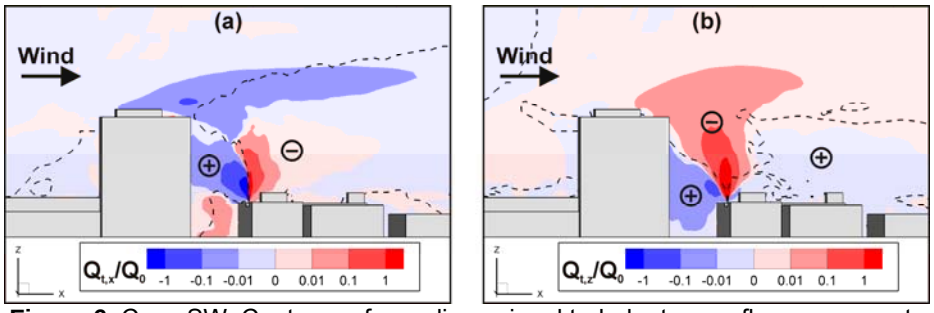

Figure 6. Case SW: Contours of non-dimensional turbulent mass flux components in the (a) streamwise and (b) vertical direction. The dashed lines represent the isolines $\partial C/\partial x_i=0$ with (a) $x_i=x$,(b) $x_i=z$. The sign of $\partial C/\partial x_i$ in the region delimited by the isoline is indicated in circles (+: positive; -: negative).

The contours of non-dimensional convective mass flux in the streamwise ($Q_{c,x}/Q_0$) and vertical ($Q_{c,z}/Q_0$) directions are shown in Figs. 5a and 5b, respectively. Fig. 5a shows that, because the source is located in the wake recirculation of the Faubourg building, pollutant is transported upstream by the backflow. This explains

the mean concentration patterns observed in the previous section. In the upper region (around Faubourg building's roof level) and farther downstream, the mean streamwise velocity is positive and carries the pollutant gas downstream ($Q_{c,x}>0$). The relatively high vertical velocity at the exhaust can be observed in Fig. 5b: the vertical convective flux is intense and reaches high values until the roof of the Faubourg building. Farther downstream, reattachment of the flow occurs, leading to negative vertical velocity and $Q_{c,z}<0$.
The contours of $Q_{t,x}/Q_0$ and $Q_{t,z}/Q_0$ are depicted in Fig. 6. In the streamwise direction (Fig. 6a), the sign of the flux is opposite to the one of $\partial C/\partial x$ in the vicinity of the stack. Hence, the gradient-diffusion (GD) hypothesis generally used with RANS models appears to be verified. At the Faubourg building roof level, $Q_{t,x}$ is opposite to $Q_{c,x}$ and is relatively less intense. In the vertical direction (Fig. 6b), the GD hypothesis is verified as well: $Q_{t,z}$ is directed from the high to low levels of mean concentration. In this direction, the convective and turbulent mass transport mechanisms act with similar intensity.

4.3 Case W: mass fluxes

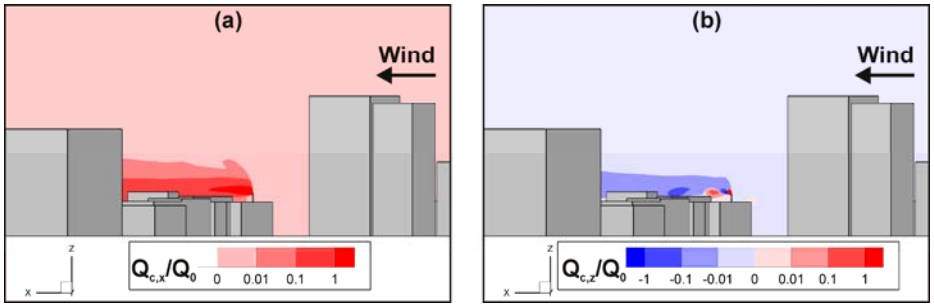

Figure 7. Case W: Contours of non-dimensional convective mass flux components in the (a) streamwise and (b) vertical direction.

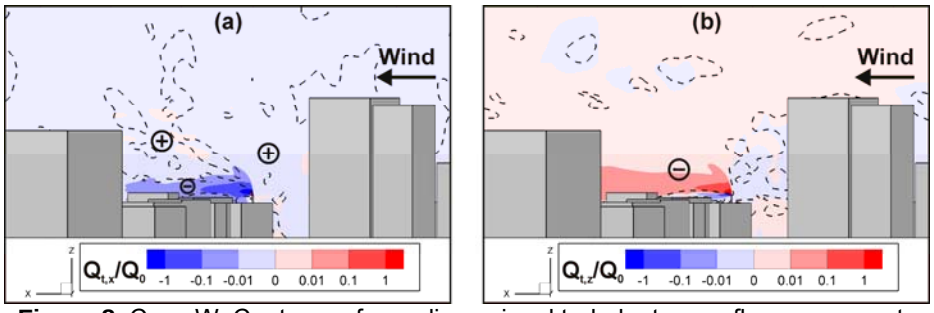

Figure 8. Case W: Contours of non-dimensional turbulent mass flux components in the (a) streamwise and (b) vertical direction. The dashed lines represent the isolines $\partial C/\partial x_i=0$ with (a) $x_i=x$,(b) $x_i=z$. The sign of $\partial C/\partial x_i$ in the region delimited by the isoline is indicated in circles (+: positive; -: negative).

Contrary to case SW, the pollutant source in case W is not located in the immediate vicinity of high-rise buildings and the plume is consequently less disturbed, as already shown in Section 4.1. No backflow is observed at the stack location and the streamwise component of the convective mass flux is therefore positive (Fig. 7a). Noticeably, the vertical velocity is negative in the plane $y=y_{stack}$ (except around the stack exhaust), leading to $Q_{c,z}<0$ (Fig. 7b). This can be explained by the reattachment of the flow downstream of the very high-rise buildings present in the upstream region of the domain (see Fig. 3).
While the mean concentration is logically decreasing from the stack exhaust towards the positive x-direction, Fig. 8a shows that the streamwise component of the turbulent mass flux is negative in this region. Thus, the counter-gradient mechanism that was observed in the case of isolated, generic buildings (Gousseau

et al. [2011b]; Rossi et al. [2010]) is also active in this case with multiple, real buildings. It is attributed to the vortical structures that are generated at the front corner of the BE building and transported in the shear layer developing above roof level. No such a singularity is observed in the vertical direction: the turbulent mass flux is directed from the high to low levels of mean concentration and the GD hypothesis is verified (Fig. 8b).

5 CONCLUSIONS

Large-Eddy Simulation of pollutant dispersion in an actual urban environment has been performed. The configuration under study involves a stack on the roof of a low-rise building in downtown Montreal, for two different wind directions (South-West and West). The focus is on the convective and turbulent mass fluxes computed by LES. The latter allow evaluating the gradient-diffusion hypothesis generally used with the RANS turbulence modelling approach for turbulent mass transport.

For case SW, the pollutant source is located in the wake recirculation zone of an upstream high-rise building. In this case, convection appears to be the dominant mechanism of mass transport in the streamwise direction, emphasizing the need for accurate prediction of the mean flowfield by the CFD model. In the vertical direction, convective and turbulent mass fluxes are of similar intensity. In both streamwise and vertical directions the turbulent mass flux is directed from the high to low levels of mean concentration, justifying the use of the gradient-diffusion hypothesis with steady models. Note that in this case the correct parameterization of the turbulent mass flux via the turbulent Schmidt number is still required.

For case W, the influence of the surrounding buildings on the dispersion is less pronounced, which can be observed by the mean concentration contours. However, the vertical convective flux is negative, suggesting the influence of the very high-rise upstream buildings on the local flow pattern around the BE building, even though they are located relatively far away from the BE building. In this case, like in the case of an isolated building in a previous study, a counter-gradient mechanism of turbulent mass transport is observed in the streamwise direction, with mass flux directed from low to high levels of mean concentration. This rather counter-intuitive result is attributed to the turbulent eddies generated at the front corner of the emitting building and transported downstream through the plume. Such a mechanism is not observed in the vertical direction and the turbulent mass flux was directed upwards. For this wind direction, the effects of convective and turbulent mass transport are opposite to each other.

By showing that the phenomena that were observed on dispersion around an isolated cubical building can also be identified for an applied case of actual urban environment, the present study demonstrates the relevance of the investigation of environmental processes on generic, simplified cases and the extrapolation of these findings to more complex, real cases.

REFERENCES

Bell, J.B., P. Colella, and H.M. Glaz, A second-order projection method for the incompressible Navier-Stokes equations, *Journal of Computational Physics, 85,* 257-283, 1989.

Fluent Inc., *Fluent 6.3 User's Guide,* 2006.

Franke, J., A. Hellsten, H. Schlünzen, and B. Carissimo, *Best practice guideline for the CFD simulation of flows in the urban environment,* COST Action 732, 2007.

Germano, M., U. Piomelli, P. Moin, and W.H. Cabot, A dynamic subgrid-scale eddy viscosity model, *Physics of Fluids, A 3,* 1760-1765, 1991.

Gousseau, P., B. Blocken, T. Stathopoulos, and G.J.F. van Heijst, CFD simulation of near-field pollutant dispersion on a high-resolution grid: a case study by LES and RANS for a building group in downtown Montreal, *Atmospheric Environment, 45,* 428-438, 2011a.

Gousseau, P., B. Blocken, and G.J.F. van Heijst, CFD simulation of pollutant dispersion around isolated buildings: on the role of convective and turbulent mass fluxes in the prediction accuracy, *Journal of Hazardous Materials, 194,* 422-434, 2011b.

Lilly, D.K., A proposed modification of the Germano subgrid-scale closure method, *Physics of Fluids, A 4,* 633-635, 1992.

Mathey, F., D. Cokljat, J.P. Bertoglio, and E. Sergent, Assessment of the vortex method for large eddy simulation inlet conditions, *Progress in Computational Fluid Dynamics, 6,* 58-67, 2006.

Moin, P., K. Squires, W. Cabot, and S. Lee, A dynamic subgrid-scale model for compressible turbulence and scalar transport, *Physics of Fluids, A3-11,* 2746-2757, 1991.

Rossi, R., D.A. Philips, and G. Iaccarino, A numerical study of scalar dispersion downstream of a wall-mounted cube using direct simulations and algebraic flux models, *International Journal of Heat and Fluid Flow, 31,* 805-819, 2010.

Smagorinsky, J., General circulation experiments with the primitive equations. I. The basic experiment, *Monthly Weather Review, 91,* 99-164, 1963.

Stathopoulos, T., L. Lazure, P. Saathoff, and A. Gupta, The effect of stack height, stack location and roof-top structures on air intake contamination - A laboratory and full-scale study, *IRSST report R-392,* 2004.

Tominaga, Y., A. Mochida, R. Yoshie, H. Kataoka, T. Nozu, M. Yoshikawa, and T. Shirasawa, AIJ guidelines for practical applications of CFD to pedestrian wind environment around buildings, *Journal of Wind Engineering and Industrial Aerodynamics, 96,* 1749-1761, 2008.

van Hooff, T. and B. Blocken, Coupled urban wind flow and indoor natural ventilation modelling on a high-resolution grid: A case study for the Amsterdam ArenA stadium, *Environmental Modelling & Software, 25,* 51-65, 2010.